ACS OMEGA

http://pubs.acs.org/journal/acsodf

Article

# Polyaniline-Coated Surface-Modified Ag/PANI Nanostructures for Antibacterial and Colorimetric Melamine Sensing in Milk Samples

Muhammad Waqas,* Luca Campbell, and Piyush T

Cite This: *ACS Omega* 2023, 8, 24010−24015

Read Online

ACCESS | Metrics & More | Article Recommendations

**ABSTRACT:** Silver nanoparticles (Ag NPs) are trusted candidates for many biological characteristics and applications due to their low toxicity and biologically benign nature. Due to inherited bactericidal characteristics, these Ag NPs are surface-modified with polyaniline (PANI), an organic polymer that has distinctive functional groups which have their role in inducing ligand properties. The Ag/PANI nanostructures were synthesized by the solution method, and their antibacterial and sensor properties were evaluated. Maximum inhibitory performance was seen with modified Ag NPs compared with their pure counterparts. The Ag/PANI nanostructures (0.1 $\mu$g) were incubated with *E. coli* bacteria, and almost complete inhibition was seen after 6 h. Furthermore, the colorimetric melamine detection assay by Ag/PANI as a biosensor also yielded efficient and reproducible results up to a 0.1 $\mu$M melamine concentration in daily-life milk samples. The chromogenic shift in color along with spectral validation through UV−vis spectroscopy and FTIR spectroscopy proves the credibility of this sensing method. Thus, high reproducibility and efficiency make these Ag/PANI nanostructures practical candidates for food engineering and biological properties.

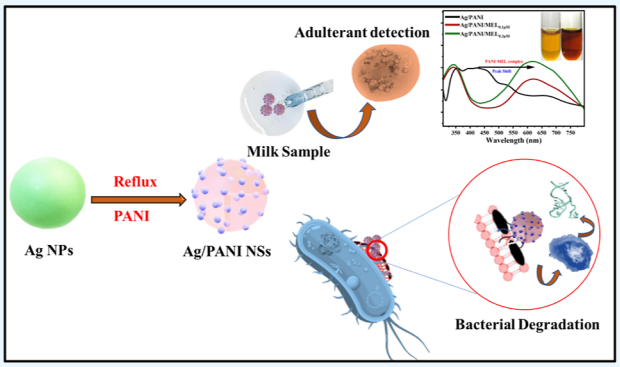


## INTRODUCTION

Currently, nanotechnology dominates the revolutionary aspects in all sectors, including pharmaceuticals,[1] environmental science,[2] energy,[3] food safety,[4] cosmetics,[5] and sensors applications.[6] At low dimensions, the inherent properties of these nanostructures are boosted, which make them best suited for these purposes. However, these characteristics of nanostructures can be tuned using coating materials, making them effective in multiple fields. Specifically, the role of nanostructures in biological viewpoints is gaining more interest because of their high activity, low toxicity,[7] and added sensing capability.[8] The intrinsic behavior of nanomaterials like silver, gold, selenium, and copper in antibacterial properties is the key aspect for using them in medicine and food storage. Scientists are considering in vitro processes to illustrate the antibacterial characteristics of these metallic NPs based on surface moieties which play a crucial role in digesting protein cell membranes. For example, plant extract-modified Se NPs were synthesized by Safdar et al., and their antibacterial properties were elaborated.[9] In a similar way, chitosan-modified ZnO nanoparticles were synthesized and enhanced antibacterial characteristics were evaluated by Alharbi et al.[10] These practices showed that the intrinsic efficiency of these metallic nanoparticles can be further improved by incorporating active organic compounds over the surface of these nanomaterials. In other words, the efficiency and diversity in applicability of these nanomaterials can be tuned using added organic polymers which functionalized the NPs' surface for real-time bioanalytics.

Additionally, the role of NPs as biosensors for different adulterants in food samples is gaining more attention for quick real-time analysis.[11] Food adulterants like melamine, salicylic acid, urea, and $H_2O_2$ are common additives in infant milk formula and food packaging materials.[12] More specifically, melamine high doses (i.e., >1 mg/kg for infant formula and >2.5 mg/kg for other dairy items) can be toxic. Therefore, determination of melamine in milk samples is a critical clinical requirement to avoid toxicity for higher melamine contents in food products. Different analytical tools are in practice to determine residual melamine contents in food samples including chromatographic processes hyphenated with advanced instruments like GC−MS, LC−MS, HPLC, bioassays, and so forth.[13] All these methods are time-consuming, tedious, nonhandy, and expensive, which makes them impractical in

**Received:** April 25, 2023
**Accepted:** June 13, 2023
**Published:** June 23, 2023

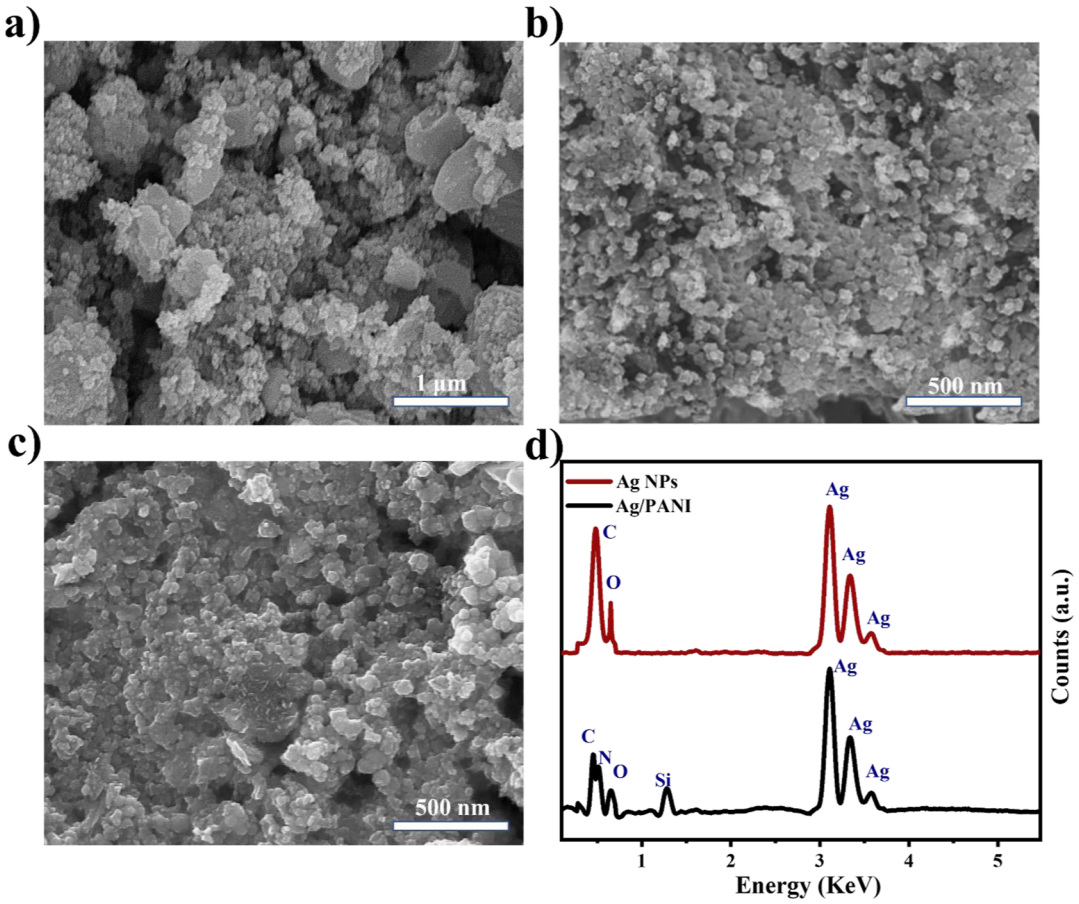


**Figure 1.** SEM images of (a,b) Ag NPs and (c) Ag/PANI nanostructures. (d) Elemental composition through EDX spectra.

real-time analytics. So, there is still room for developing on-time probes for investigating adulterant contents in food samples. Nanomaterial-based biosensors are considered novel design materials for quick, efficient, and precise melamine determination. The spectral analysis (UV−vis spectroscopy) supplies both qualitative and quantitative information in less time. Yuan et al. synthesized $MnO_2$-modified Au NPs for colorimetric detection of melamine in biological assays up to a 16 nM concentration.[14] The group illustrated a single-atom probe for melamine detection by surface binding of gallic acid with melamine which supplied the basics for color formation. Following the sequence, Affrald et al. developed alginate-modified gold NPs as biosensors for melamine detection.[15] The precision and reproducibility of these NP-based nanosensors urged the development of new systematic tools for enhanced applications in in-field real-time analytics.

Polyaniline (PANI), an organic polymer, has crucial properties that boost the stability and key characteristics of NPs when it binds to metallic sites. Moreover, PANI has a conjugative structure with different binding groups which can sustain different functional groups in sample media and provide biosensor applicability by binding with targeted molecules. For instance, researchers have developed PANI-based biosensors for in situ determination of food adulterants in milk samples.[16] The binding sites residing in the PANI molecule form a chemical linkage with adulterants, and new complex formation provides the basics for spectral determination of specific analytes in the sample.

Herein, we synthesized PANI-coated Ag nanoparticles (Ag/PANI) for enhanced in situ stability and functionality toward antibacterial activity and colorimetric detection of melamine in domesticated pretreated milk samples. Surface-modified Ag NPs have high in situ reproducibility and specificity for melamine detection.

## METHODS

**Experimental Section.** *Materials.* Silver nitrate ($AgNO_3$), ascorbic acid, ethylene glycol ($C_2H_6O_2$), sodium citrate ($C_6H_5Na_3$), melamine, PANI, trichloroacetic acid, NaOH, and ethanol were the chemicals used.

*Synthesis of Ag NPs.* Ag NPs were synthesized by a typical one-pot chemical reduction method using 2 aliquots of 5 mL of EG containing $AgNO_3$ (190 mM) and ascorbic acid (140 mM) separately. The solution holding $AgNO_3$ in EG was refluxed at 80 °C, and an ascorbic acid solution was added dropwise into this. The color changes from yellow to light brown within 10 min indicated the formation of Ag NPs. The solution was then suddenly cooled to room temperature to avoid larger grain size and centrifuged at 4500 rpm. The precipitates were then washed with deionized water (18.2 MΩ Milli-Q) and then with absolute ethanol to remove residual impurities. The obtained NPs were then dried at 50 °C overnight.

**Synthesis of Modified Ag/PANI Nanoparticles.** The PANI-modified Ag NPs were synthesized using the same method. Ascorbic acid was replaced with PANI (0.1 M), and after mixing the two solutions, the mixture was refluxed at 80 °C for 30 min. The dark-brown residue was then centrifuged, washed thrice with ethanol, and dried at 50 °C overnight.


https://doi.org/10.1021/acsomega.3c02627
ACS Omega 2023, 8, 24010−24015

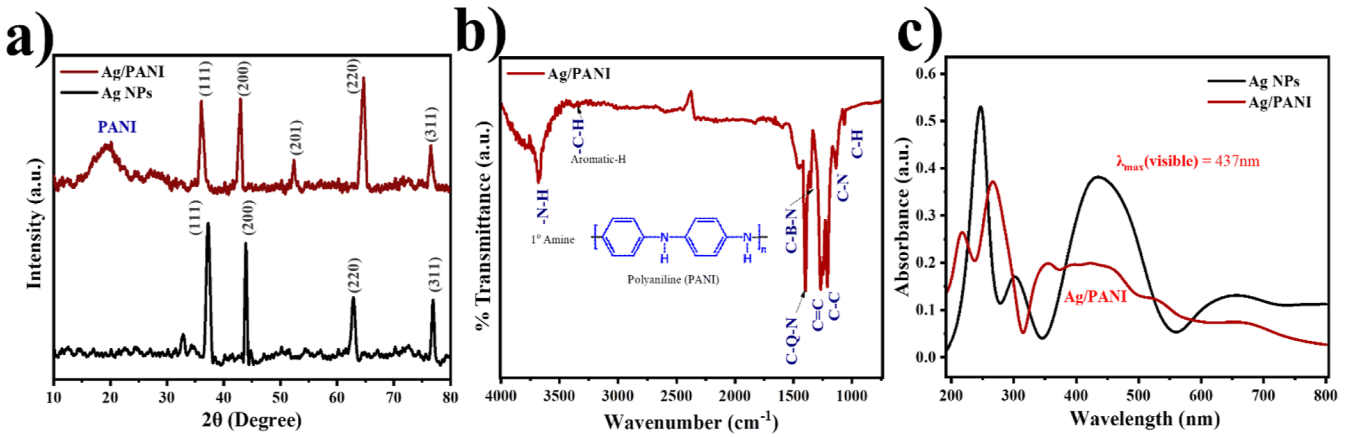


**Figure 2.** (a) XRD spectra of Ag NPs and Ag/PANI nanostructures, (b) FTIR spectra of Ag/PANI nanostructures, and (c) UV−vis spectra of Ag NPs and Ag/PANI nanostructures.

*Characterization.* The synthesized Ag NPs and surface-modified Ag/PANI nanostructures were characterized using UV−vis spectroscopy (UV−vis-Evolution-300, wavelength range from 190 to 800 nm), scanning electron microscopy (SEM) (LEO S430), coupled with energy-dispersive X-ray spectroscopy (EDX) and X-ray diffraction (XRD) (Bruker-D8 Transit diffractometer).

**Antibacterial Analysis.** *Bacterial Strain Formulation.* The synthesized Ag NPs and surface-modified Ag/PANI nanostructures were tested against the *E.coli* Gram-negative bacterial strain (i.e., NCTC8196). Before testing, the strains were stored at −70 °C in a culture medium containing Luria−Bertani broth. The active bacterial strain was then cultured in nutrient agar broth at 36.5 °C for 1 day.

*Optical Density Growth Curves of E. Coli Cultured against Ag NPs and Surface-Modified Ag/PANI Nanostructures.* Growth curves for determination of bacterial cell population kinetics exposed to Ag NPs and Ag/PANI nanostructures were evaluated at different time intervals. In a typical method, an assembly of 96-well plates was supplemented with 250 μL of a solution holding both NPs (0.1 μg) and *E.coli* bacterial strains. Optical density (OD) tests were conducted at 0, 2, 4, 6, 12, and 24 h time intervals at a typical UV−vis wavelength of 600 nm. The control test was also performed without NP inoculation in the sample medium.

**Colorimetric Method for Melamine Detection.** The pretreated milk sample taken from the local market was subjected to the typical concentration of Ag/PANI NPs. The pretreatment was done according to a general process[17] in which an aliquot of 5 mL of liquid milk was taken into a centrifuge tube and added with 1.5 mL of 300 g/L trichloroacetic acid. The solution was then vortexed for 1 min, and agglomerated proteins were skimmed off the centrifuge tube after 4 min of sonication and 5 min of centrifugation at 11,000 rpm. The clear supernatant was then adjusted to pH 7 by adding drops of a 1 M NaOH solution. Furthermore, the solution was filtered through a Whatman filter paper (0.22 mm). This solution (10 mL) was then treated with 5 mL of surface-modified Ag/PANI nanostructures (light brown) and sonicated for 10 min. Then, this solution was warmed up to 40 °C for 3 min until a color change appeared from light brown to reddish brown. The absorption spectra were then taken for different concentrations of melamine in the milk sample. The limit of detection and linear range were estimated against different concentrations of standard melamine solutions (i.e., $10^{-5}$ to $10^{-2}$ g/L).

## RESULTS AND DISCUSSION

The morphological aspects were considered through SEM analysis which depicts microspheres like Ag nanoparticles (Figure 1a,b). The high-magnification SEM image showed that Ag NPs have an average diameter of ∼80 nm. The spherically shaped NPs were uniformly dispersed throughout the phase structure which describes the suitability of the synthetic route. Similarly, the surface-modified Ag/PANI nanostructures depicted a diffused morphology where Ag nanoparticles seemed to be coated by PANI molecules uniformly (Figure 1c). Although surface modification somehow agglomerated the Ag NPs, there was negligible change in the average diameter and shape of Ag/PANI nanostructures. The SEM analysis was coupled with EDX which describes the elemental composition of both Ag NPs and Ag/PANI nanostructures (Figure 1d). The EDX spectra clearly reveal the elemental composition of Ag NPs with a Ag percentage of ∼87%, while in the case of Ag/PANI, the N along with the C peak appeared, which indicates carbon and nitrogen contents of PANI.

The structural and phase characteristics of Ag NPs and Ag/PANI nanostructures were explored through XRD (Figure 2a). The XRD spectra of Ag NPs confirm formation of the face-centered cubic symmetry of Ag NPs with diffraction peaks at 38, 44, 64, and 77° corresponding to the lattice planes (111), (200), (202), and (311), respectively (JCPDS card no. 04-0783). In the case of Ag/PANI, the XRD analysis showed a broad peak range of ∼15−25° which depicts the noncrystalline PANI phase over Ag NPs. The diffraction peaks at (111), (200), and (311) for Ag NPs slightly shifted to lower angles with a lower intensity, which further validates PANI residues coated over Ag NPs.

Surface functionalities of modified Ag/PANI nanostructures were explored using Fourier transform infrared (FTIR) spectroscopy. The high-intensity transmittance peak along with vicinal shoulder peaks at 1398 and 1358 $cm^{-1}$ corresponds to stretching vibrations of quinoid and benzenoid functionalities of aromatic amines, respectively (Figure 2b). The peaks at 1059 and 1129 $cm^{-1}$ correspond to out-of-bending vibrations of aromatic-H and C−N bonds. C═C and C−C peaks appeared at 1200 and 1257 $cm^{-1}$, respectively, revealing aromatic conjugated structures of PANI. A slightly


https://doi.org/10.1021/acsomega.3c02627
ACS Omega 2023, 8, 24010−24015

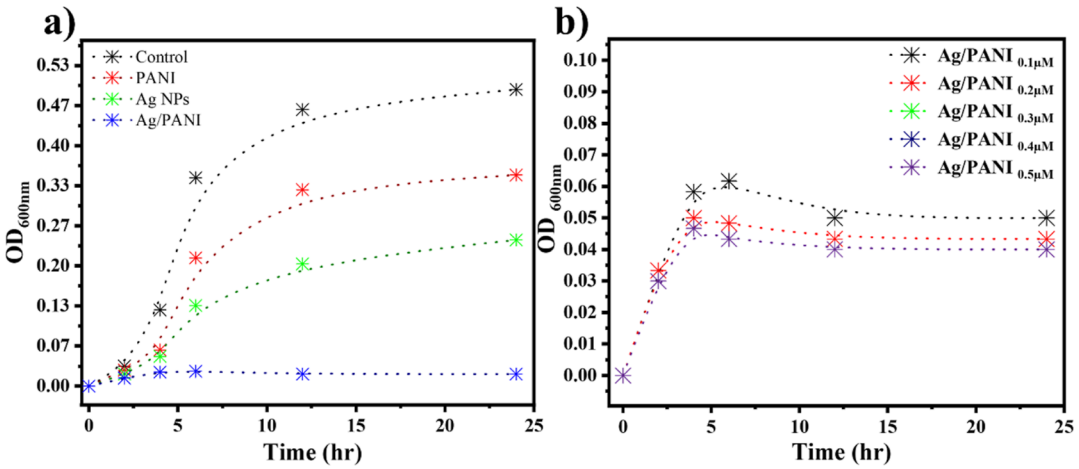


**Figure 3.** (a) Kinetics of bacterial growth against PANI, Ag NPs, and the Ag/PANI hybrid through OD curves at 600 nm. (b) OD curves for different concentrations of Ag/PANI nanostructures.

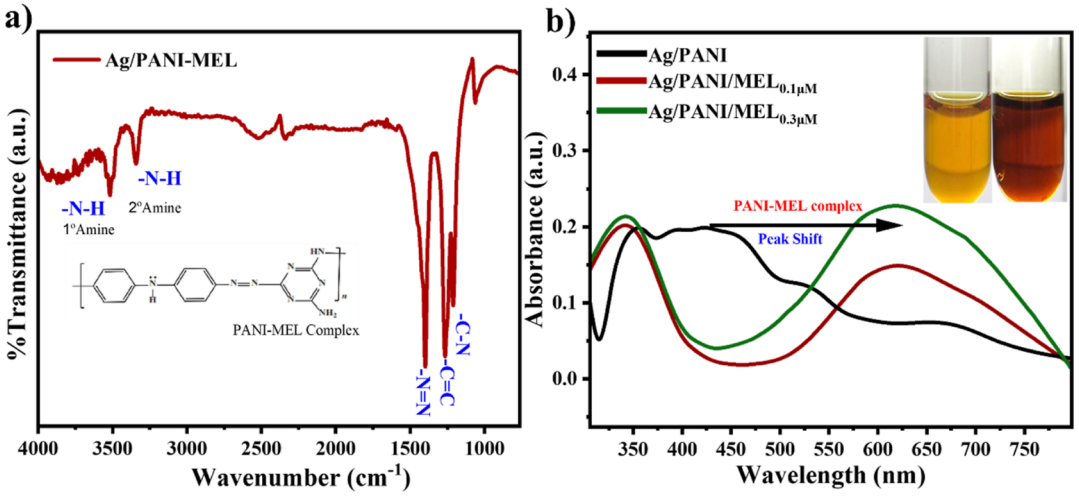


**Figure 4.** (a) FTIR spectra of the PANI−MEL complex for colorimetric melamine sensing and (b) chromogenic band shift determination via UV−vis spectra.

broad stretching vibration peak for 1° amine (−N−H) appeared at 3877 $cm^{-1}$ along with an aromatic-H stretching vibration peak just above 3000 $cm^{-1}$. These surface groups clearly illustrate the PANI coating over Ag NPs.

The UV−vis absorption spectra of Ag NPs along with Ag/PANI nanostructures show the position of plasmon absorption for pure Ag and surface-modified Ag NPs. The intense broad peak with an absorption maximum at 437 nm confirms spherically shaped Ag NPs (Figure 2c). The literature reveals that anisotropic particles could have more than one surface plasmon resonance (SPR) band depending upon the shape and size of the particles. However, clearly, a single broad SPR band is present in the UV−vis spectra of pure Ag NPs. In contrast, UV−vis spectra of Ag/PANI nanostructures reveal a multiband spectrum with a blue shift in the absorption maxima ∼415 nm due to surface moieties which can shift the absorption coefficient toward lower wavelengths.

**Antibacterial Mechanism of Action.** Antibacterial characteristics of Ag NPs and PANI-modified Ag/PANI nanostructures were depicted through inhibited growth patterns drawn by the OD method. The comparative bactericidal activities were tested by incubating *E.coli* strains against the same concentrations (i.e., 0.1 $\mu$m) of PANI, pure Ag NPs, and Ag/PANI nanostructures (Figure 3a). The control (no bactericidal agent) was also taken to explain the role of metal nanostructures in bactericidal properties. OD kinetics curves reveal a modest reduction of PANI and pure Ag NPs in culture colonies as compared with Ag/PANI nanostructures. There is a slight increase in the growth curve up to 4 h, but then almost complete inhibition was observed after 6 h. Rapid interaction of reactive amine groups of PANI with oxygen-containing groups of lipopolysaccharides (the active component of the cell membrane) can be explained. This provides a pathway for attachment of Ag/PANI nanostructures with the cell membrane of bacteria. Inhibition occurs when Ag NPs encounter the replicates of genetic structure (i.e., RNA) which further leads to its bactericidal property. Thus, PANI facilitates the infusibility of Ag NPs in bacterial cells by ingesting the cell membrane. In comparison, pure Ag NPs possess an infusibility barrier which limits the activity of these NPs.

The reactivity of Ag NPs was enhanced by surface-coated PANI which causes rapid degeneration of the bacterial cell membrane to facilitate the attack of Ag with the genetic structures of bacteria. Different molar concentrations (i.e., 0.2, 0.3, 0.4, and 0.5 $\mu$m) of Ag/PANI were tested to further


https://doi.org/10.1021/acsomega.3c02627
ACS Omega 2023, 8, 24010−24015

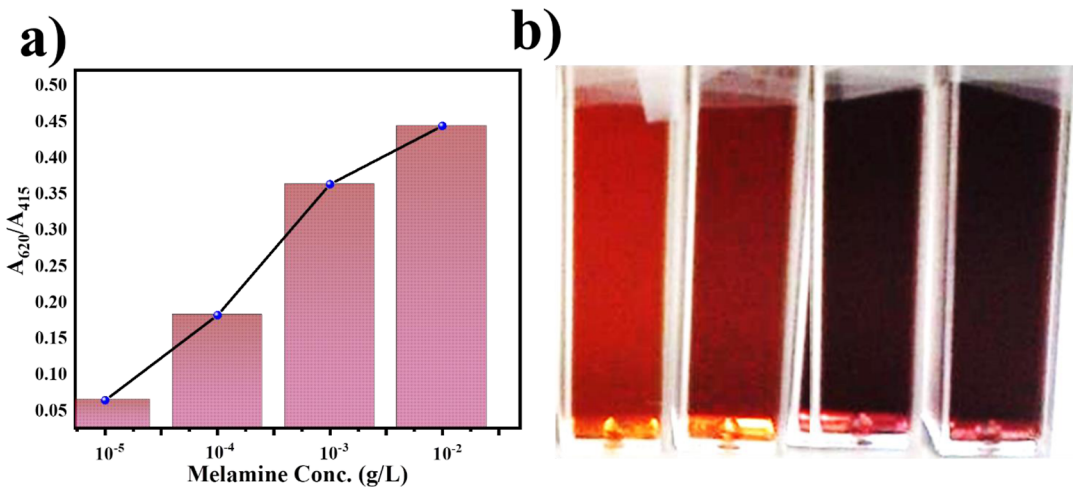


**Figure 5.** (a) $A_{620}/A_{415}$ absorption ratio and (b) chromogenic band shift photograph for different melamine concentrations.

explore the inhibitory effect of these nanostructures (Figure 3b). It can be seen through OD kinetic curves that, beyond 0.3 $\mu$m, no further inhibition was observed, which can be explained by site-specific attachment of the PANI molecule.

**Melamine Detection Assay.** The colorimetric detection of melamine in the milk sample was evaluated by the change in color of the sample solution. Further validation was done through FTIR analysis which provides information about changes in chemical linkages and corresponding functional group variations. The basics of melamine detection lie in the bond formation of aniline with melamine. This linkage yields secondary amine when PANI−MEL are linked together. This can be described by FTIR stretching peaks at 3338 and 3518 $cm^{-1}$ which correspond to 2 and 1° amines (−N−H), respectively (Figure 4a). The Ag/PANI linkage is further confirmed by the color change from brownish to reddish brown.

The limit of detection and linear range sensitivity were estimated up to $10^{-6}$ g/L using UV−vis spectroscopy. The $A_{620}/A_{415}$ ratio was taken with different standard doses of melamine. The sensitivity of Ag/PANI nanostructures was less affected with lower concentrations of melamine when $A_{620}/A_{415}$ was increased from $10^{-5}$ to $10^{-2}$ g/L (Figure 5a,b). The spectral evidence further validates the red shift in SPR, and a broad peak emerges between 470 and 765 nm.

This shift in absorption was due to the PANI−MEL complex which shifts the absorption coefficient of Ag NPs toward higher wavelengths. This is due to Ag NP aggregation and diazo bond formation in the PANI−MEL complex. The process is further extended for higher concentrations of melamine which yielded reproducible results, which proved the efficacy of the method.

## CONCLUSIONS

In this study, Ag NPs and surface-modified Ag/PANI nanostructures were synthesized by the chemical reduction method. PANI as a coating material induced enhanced bactericidal properties of Ag NPs compared with pristine inherited antibacterial efficacy of both pure Ag NPs and PANI molecules. The inhibited growth kinetics was evaluated through OD curves which showed almost complete inhibition of *E.coli* bacteria. This enhanced antibacterial activity is due to high surface kinetics and rapid attachment over bacterial cell membranes due to the lipopolysaccharide linkage between PANI and membrane constituents. Moreover, colorimetric melamine detection by surface PANI-linked Ag NPs is another applicability. This chromogenic shift from brown to reddish brown color gave the basics of the melamine detection assay. Melamine detection up to 0.1 $\mu$M in milk samples with reproducible results confirmed the applicability of these nanostructures in real-time food analysis. Also, these nanostructures can be used for electrochemical sensing of different food adulterants in on-time investigations.

## AUTHOR INFORMATION

### Corresponding Author

**Muhammad Waqas** − *Institute of Chemical Sciences, Bahauddin Zakariya University, Multan 59300, Pakistan;* orcid.org/0000-0001-7305-9423; Email: mwaqas.k@yahoo.com

### Authors

**Luca Campbell** − *Lovejoy High School, Lucas, Texas 75002, United States*

**Piyush T** − *Institute of Electric and Electronic Engineers, New York, New York 10016, United States*

Complete contact information is available at: https://pubs.acs.org/10.1021/acsomega.3c02627

### Notes

The authors declare no competing financial interest.

## REFERENCES

(1) Hamida, R. S.; Ali, M. A.; Alfassam, H. E.; Momenah, M. A.; Alkhateeb, M. A.; Bin-Meferij, M. M. One-Step Phytofabrication Method of Silver and Gold Nanoparticles Using Haloxylon Salicornicum for Anticancer, Antimicrobial, and Antioxidant Activities. *Pharmaceutics* **2023**, *15*, 529.

(2) Sampath, G.; Govarthanan, M.; Rameshkumar, N.; Vo, D.-V. N.; Krishnan, M.; Sivasankar, P.; Kayalvizhi, N. Eco-friendly biosynthesis metallic silver nanoparticles using Aegle marmelos (Indian bael) and its clinical and environmental applications. *Appl. Nanosci.* **2023**, *13*, 663−674.

(3) Kanti Das, S.; Chatterjee, S.; Banerjee, A.; Kumar, G.; Kumar Patra, A.; Sundar Dey, R.; Pal, A. J.; Bhaumik, A. A novel chemical approach for synthesizing highly porous graphene analogue and its composite with Ag nanoparticles for efficient electrochemical oxygen reduction. *Chem. Eng. J.* **2023**, *451*, 138766.



https://doi.org/10.1021/acsomega.3c02627
*ACS Omega* 2023, 8, 24010−24015

(4) Ventura-Aguilar, R. I.; Bautista-Baños, S.; Mendoza-Acevedo, S.; Bosquez-Molina, E. Nanomaterials for designing biosensors to detect fungi and bacteria related to food safety of agricultural products. *Postharvest Biol. Technol.* **2023**, *195*, 112116.
(5) Keskin, M.; Kaya, G.; Bayram, S.; Kurek-Górecka, A.; Olczyk, P. Green Synthesis, Characterization, Antioxidant, Antibacterial and Enzyme Inhibition Effects of Chestnut (Castanea sativa) Honey-Mediated Silver Nanoparticles. *Molecules* **2023**, *28*, 2762.
(6) Sudarman, F.; Shiddiq, M.; Armynah, B.; Tahir, D. Silver nanoparticles (AgNPs) synthesis methods as heavy-metal sensors: a review. *Int. J. Environ. Sci. Technol.* **2023**, 1−18.
(7) Tortella, G.; Rubilar, O.; Durán, N.; Diez, M.; Martínez, M.; Parada, J.; Seabra, A. Silver nanoparticles: Toxicity in model organisms as an overview of its hazard for human health and the environment. *J. Hazard Mater.* **2020**, *390*, 121974.
(8) Jayarambabu, N.; Saraswathi, K.; Akshaykranth, A.; Anitha, N.; Venkatappa Rao, T.; Rakesh kumar, R. Bamboo-mediated silver nanoparticles functionalized with activated carbon and their application for non-enzymatic glucose sensing. *Inorg. Chem. Commun.* **2023**, *147*, 110249.
(9) Safdar, M.; Aslam, S.; Akram, M.; Khaliq, A.; Ahsan, S.; Liaqat, A.; Mirza, M.; Waqas, M.; Qureshi, W. A. Bombax ceiba flower extract mediated synthesis of Se nanoparticles for antibacterial activity and urea detection. *World J. Microbiol. Biotechnol.* **2023**, *39*, 80.
(10) Alharbi, R. A.; Alminderej, F. M.; Al-Harby, N. F.; Elmehbad, N. Y.; Mohamed, N. A. Design, Synthesis, and Characterization of Novel Bis-Uracil Chitosan Hydrogels Modified with Zinc Oxide Nanoparticles for Boosting Their Antimicrobial Activity. *Polymers* **2023**, *15*, 980.
(11) (a) Kumar, S.; Sharma, R.; Bhawna; Gupta, A.; Singh, P.; Kalia, S.; Thakur, P.; Kumar, V. Prospects of Biosensors Based on Functionalized and Nanostructured Solitary Materials: Detection of Viral Infections and Other Risks. *ACS Omega* **2022**, *7*, 22073−22088. (b) Yang, Y.; Zhai, S.; Liu, C.; Wang, X.; Tu, Y. Disposable immunosensor based on electrochemiluminescence for ultrasensitive detection of ketamine in human hair. *ACS Omega* **2019**, *4*, 801−809.
(12) Zhang, H.; Wu, Z.; Zhi, Z.; Gao, W.; Sun, W.; Hua, Z.; Wu, Y. Practical and Efficient: A Pocket-Sized Device Enabling Detection of Formaldehyde Adulteration in Vegetables. *ACS Omega* **2021**, *7*, 160−167.
(13) Qiu, J.; Chu, Y.; He, Q.; Han, Y.; Zhang, Y.; Han, L. A self-assembly hydrophobic oCDs/Ag nanoparticles SERS sensor for ultrasensitive melamine detection in milk. *Food Chem.* **2023**, *402*, 134241.
(14) Yuan, X.; Zhang, H.; Yuan, X.; Mao, G.; Wei, L. Single particle detection based colorimetric melamine assay with MnO2-modified gold nanoparticles. *Microchem. J.* **2023**, *184*, 108133.
(15) Affrald, R. J.; Banu, S. P. N.; Arjunan, D.; Selvamani, K. A.; Narayan, S. Synthesis and Characterisation of Alginate Functionalized Gold Nanoparticles for Melamine Detection. *J. Bionanosci.* **2023**, *13*, 145−152.
(16) Singh, A. K.; Singh, M.; Verma, N. Electrochemical preparation of Fe 3 O 4/MWCNT-polyaniline nanocomposite film for development of urea biosensor and its application in milk sample. *J. Food Meas. Char.* **2020**, *14*, 163−175.
(17) Aftab, R.; Ahsan, S.; Liaqat, A.; Safdar, M.; Chughtai, M. F. J.; Nadeem, M.; Farooq, M. A.; Mehmood, T.; Khaliq, A. Green-synthesized selenium nanoparticles using garlic extract and their application for rapid detection of salicylic acid in milk. *Food Sci. Technol.* **2023**, *43*, 43.


https://doi.org/10.1021/acsomega.3c02627
*ACS Omega* 2023, 8, 24010−24015